Periodic Disturbance Compensation Using State-Space Servo Control Based on Numerical Modeling

Michael E. Aiello

Version 1.1, July 25, 2021

Keywords: Numerical methods, State-Space, Disturbance compensation, Servo control, DC bus ripple and droop rejection

Abstract

Traditional State-Space Servo control involves the use of D/Q transformations to create a simplified set of equations for the control of a servo motor in the *stationary* plane of reference. While providing simplicity in the calculations for control of the motor, this approach forces the assumption of a motor model having a completely balanced parameter set. This short presentation will show that with a modest increase in calculation overhead, a state space approach can be utilized without transformations, allowing all parameters of the motor model to be used in the control system. This allows full control of the a motor with an unbalanced parameter set. A method to cancel the effects of DC bus ripple voltage on the voltage applied to the motor is also presented.

1 Introduction

Given a reference generator that can produce a desired trajectory consisting of commands θ_d, ω_d, α_d and $\dot{\alpha_d}$, the equations for a *balanced* feed-forward portion of a State-Space controller can be produced with the equations listed in Equations 1 through 6 (see Figure 1 below).

$$i_{dd}(\omega_d) = -\frac{N_r L K_m \omega_d^2}{R^2 + (N_r \omega_d L)^2} \tag{1}$$

$$i_{qd} = \frac{J}{K_m}\alpha_d + \frac{B}{K_m}\omega_d \tag{2}$$

$$\frac{di_{dd}}{dt}(\omega_d) = -\frac{2N_r L K_m R^2 \omega_d \alpha_d}{R^2 + (N_r \omega_d L)^2} \tag{3}$$

$$\frac{di_{qd}}{dt} = \frac{J}{K_m}\dot{\alpha_d} + \frac{B}{K_m}\alpha_d \tag{4}$$

$$v_{dd} = L\frac{di_{dd}}{dt} + Ri_{dd} - N_r \omega_d L i_{qd} \tag{5}$$

$$v_{qd} = L\frac{di_{qd}}{dt} + Ri_{qd} + N_r \omega_d L i_{dd} + K_m \omega_d \tag{6}$$

Figure 1: Reference generation for State-Space control based on the D/Q *stationary* reference. (Reference paper [1] and paper [2], Appendix B.)

A numerical equivalent for Equations 1 through 6 can be generated as follows which provides an equivalent and can be used to describe an *unbalanced* system.

First, a group of equations needs to be solved numerically.

$$L_a\frac{\Delta i_{ad}}{\Delta t_h} - M_{ab}\frac{\Delta i_{bd}}{\Delta t_h} - M_{ac}\frac{\Delta i_{cd}}{\Delta t_h} = v_{ad} - R_a i_{ad} + K_a\omega_d \sin(N_r\theta_d) \quad (7)$$

$$-M_{ab}\frac{\Delta i_{ad}}{\Delta t_h} + L_b\frac{\Delta i_{bd}}{\Delta t_h} - M_{bc}\frac{\Delta i_{cd}}{\Delta t_h} = v_{bd} - R_b i_{bd} + K_b\omega_d \sin(N_r\theta_d - 2\pi/3) \quad (8)$$

$$-M_{ac}\frac{\Delta i_{ad}}{\Delta t_h} - M_{bc}\frac{\Delta i_{bd}}{\Delta t_h} + L_c\frac{\Delta i_{cd}}{\Delta t_h} = v_{cd} - R_c i_{cd} + K_c\omega_d \sin(N_r\theta_d - 4\pi/3) \quad (9)$$

$$\begin{aligned} J_m\alpha_d = -B_m - K_a i_{ad}\sin(N_r\theta_d) - K_b i_{bd}\sin(N_r\theta_d - 2\pi/3) \\ -K_c i_{cd}\sin(N_r\theta_d - 4\pi/3) \end{aligned} \quad (10)$$

$$i_{ad}\cos(N_r\theta_d) + i_{bd}\cos(N_r\theta_d - 2\pi/3) + i_{cd}\cos(N_r\theta_d - 4\pi/3) = i_{dd} \quad (11)$$

$$i_{ad} + i_{bd} + i_{cd} = 0 \quad (12)$$

Figure 2: Reference generation for State-Space control based on a numerically derived *rotating* reference.

Referring to Figure 2 above, $\Delta i_{xd} = i_{xd} - i_{xd_{prev}}$ with Δt_h the servo update rate of 50 uSec. The terms ω_d, θ_d, i_{dd}[1],Δt_h and $i_{xd_{prev}}$ are considered constant over one servo cycle allowing equations 7 through 12 to be solved for i_{ad}, i_{bd}, i_{cd}, v_{ad}, v_{bd} and v_{cd} using Gaussian elimination.

We now recompute v_{dd} and v_{qd} as shown in Figure 3 below.

$$v_{ad}\cos(N_r\theta_d) + v_{bd}\cos(N_r\theta_d - 2\pi/3) + v_{cd}\cos(N_r\theta_d - 4\pi/3) = v_{dd} \quad (13)$$

$$-v_{ad}\sin(N_r\theta_d) - v_{bd}\sin(N_r\theta_d - 2\pi/3) - v_{cd}\sin(N_r\theta_d - 4\pi/3) = v_{qd} \quad (14)$$

Figure 3: Recalculation of v_{dd} and v_{qd} based on numerical the calculations of v_{ad}, v_{bd} and v_{cd} in Figure 2 above.

[1]Here i_{dd} is derived from Equation 1

To satisfy the calculation needed to compute the error equation for the State-Space controller (See Equation 43 of [2], Appendix B), we must also recompute i_{qd} as shown in Figure 4 below.

$$-i_{ad}\sin(N_r\theta_d) - i_{bd}\sin(N_r\theta_d - 2\pi/3) - i_{cd}\sin(N_r\theta_d - 4\pi/3) = i_{qd} \qquad (15)$$

Figure 4: Recalculation of i_{qd} based on numerical calculations of $_{ad}$, i_{bd} and i_{cd} in Figure 2 above.

Equations 13, 14, 15 with θ_d and ω_d now allows us to control the *un-balanced* motor since we now have parameters K_a, K_b, K_c, L_a though M_{bc}, and R_a, R_b, R_c exposed in the representation of the system. We also have the ability to model phase shift errors in sin() and *cos*() terms.

In addition, the sin() and cos() terms can be replaced with trapezoidal terms analogous to that represented by DC Brush-less motors. Doing so here is beyond the scope of this document.

2 Conditions For This Experiment

Before continuing, an explanation for the conditions used to run this simulation needs to presented. These conditions are:

- The background information for how this simulation was created is present in this paper [2] with the following references.
- The equations for the motor used in the simulation is presented in Equation (10) of this paper.
- Application of the motor voltages was produced using *minus side clamped* Space-Vector PWM operating at 20 KHz as presented in Figures 11, 13, 14. 26 and 28 of this paper.
- A plot of ω_d vs the actual motor generated ω is shown in Figure 32 of this paper. It's important to note that there was no State-Space error compensation preformed in this simulation. So it can be noticed that two signals do not track exactly as shown in Figure 32. However, it will be a requirement for the demonstration provided in this paper that a *weak* compensation for position error must be performed for at least two of the three tests presented below. This is because for the numerical model generated reference described in Equation 7 through 12 above, motor position must track the generated reference position with minimal error. To do this, I used only a *position error* compensation of $(thetad - theta) * 40.0$ added to the v_{qd} terms described by Equations 6 and 14 to keep tracking of position under control without affecting in any significant way the parameter imbalances injected into the system.
- Parameter values for K_a, K_b, L_a and so forth used in Equations 7 through 12 above are provided in Table 3 of this paper (note typo,. should be titled **Servo Motor Parameters**). In addition note that values for M_{ab}, M_{bc} and so forth were set at 93 percent of L. The demonstration below will show the effects of the simulation when these values are set for an unbalanced state (e.g. K_a != K_b != K_b, ... M_{ab} != M_{bc} and so forth).
- The trajectory for generating θ_d, ω_d and so forth is based on a sinusoidal ramping function. The author acknowledges that this generator should have been based on sigmoid functions.
- Simulation time runs from 0 to 1 second for each test. The trajectory generator and the equations that control the State-Space reference run at a rate of 20 KHz. The ODE equations for the simulation run at pseudo-realtime using a sixth order Runge-Kutta interpolation having a minimum time step of 1 nSec and a maximum of 200 nSec.

Before introducing imbalances into the motor model, it must be shown that there is an equivalence between the traditional D/Q based reference and that which is derived numerically. This is shown in Figures 5 and 6 below based on the acceleration plots of *desired* and *actual*. With a perfectly balanced motor model, the two plots match with one exception.

The reader may notice a slighte *fuzzy* look on α (alpha) of Figure 5 relative to Figure 6 for the same signal. This may be due to the fact that the D/Q based (analytical) reference is generated using $\dot{\alpha_d}$ (beta) at 20 KHz. This is not

the case with the numerical based reference whose highest order differentiation of position is α_d (alpha)[2].

This may be an additional benefit for using the numerical method over the analytical approach. However, this anomaly is unrelated to the tests that are about to be presented.

[2] At this point I have not investigated this to verify that this is the problem

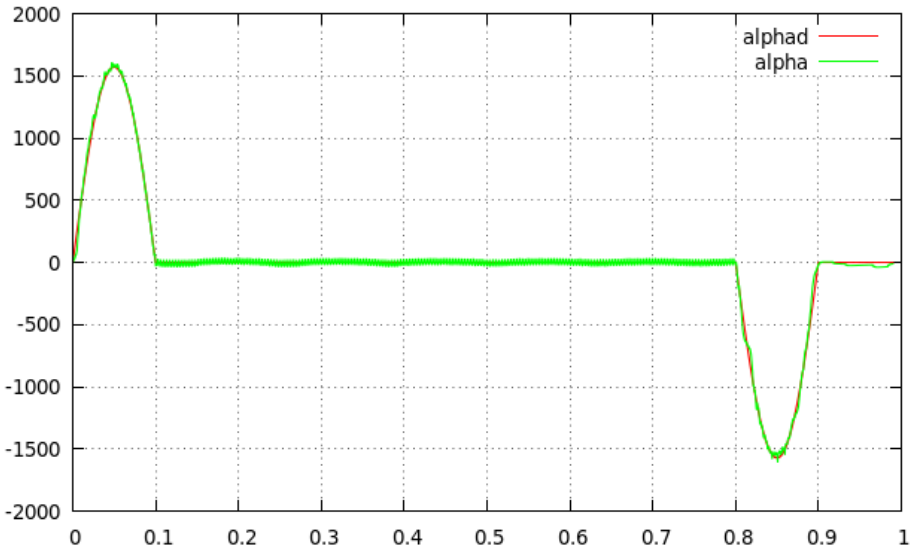

Figure 5: Plot of α_d vs motor α using analytical D/Q State-Space reference generation described by Equations 1 through 6.

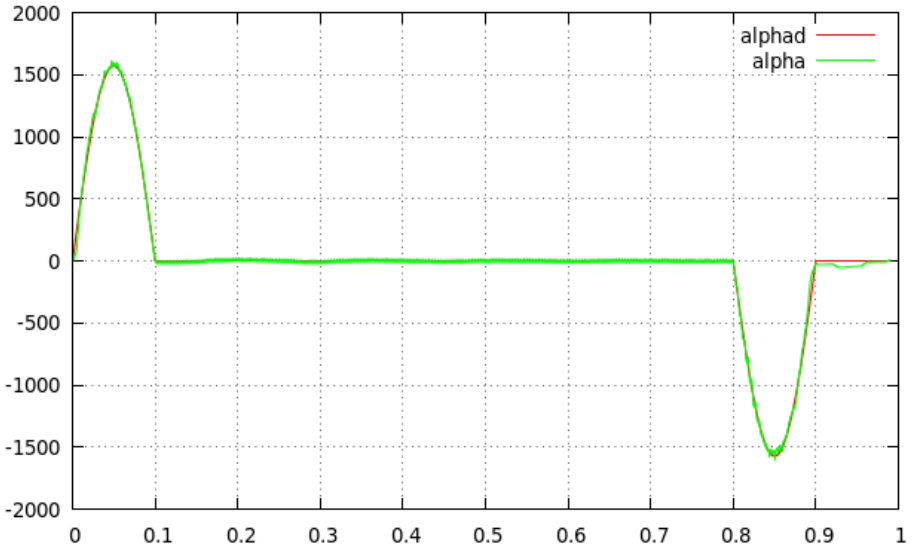

Figure 6: Plot of α_d vs motor α using a numerical State-Space reference generation described by Equations 7 through 12.

3 Periodic Disturbance Compensation Test

A test is setup to see how well the numerically generated reference performs over the analytical reference when adding imbalances to three phase specific parameters of the motor model.

For both tests I modify the motor equations as follows (See Equation 10 of [2]).

- A change of torque constant K_b to .13. K_a and K_c remain .1 N*m/amp.
- A change of mutual inductance M_{ac} to .2e-3. M_{ab} and M_{bc} remain at .495e-3 henrys.
- A change to the position relationship of Phase B with respect to Phase A and C. Phase B becomes $sin(Nr * theta + .05 * PI - 2 * PI/3)$ while Phase A and C remain $sin(Nr * theta)$ and $sin(Nr * theta - 4 * PI/3)$ respectively.

Next, the same modifications listed above (for the motor) are also done to the set of numerical Equations 7 through 12 above.

Now note that for the analytical reference model described by Equations 1 through 6 above, these modifications cannot be made because the use of D/Q transformations has made these *phase specific* parameters hidden from the control system.

The results of this test are as follows.

Figure 7 shows the acceleration plot of the motor controlled by the D/Q based reference model. Significant ripple exists on the motor acceleration.

Figure 8 portrays the motor acceleration plot using the numerical based reference model. It can be noted the dramatic reduction of acceleration ripple relative to the acceleration command reference $alpha_d$.

Correspondingly, one can also see these effects by the monitoring torque component of the motor voltage command (signal v_{qd}).

For the D/Q based reference, Figure 9 shows no corresponding ripple for the simple reason that Equations 1 through 6 were not (and could not) be modified to cancel the imbalances added to the motor model. On the other hand, Figure 10 does exhibit the *imbalance canceling* ripple created by adding the imbalances to Equations 7 through 12.

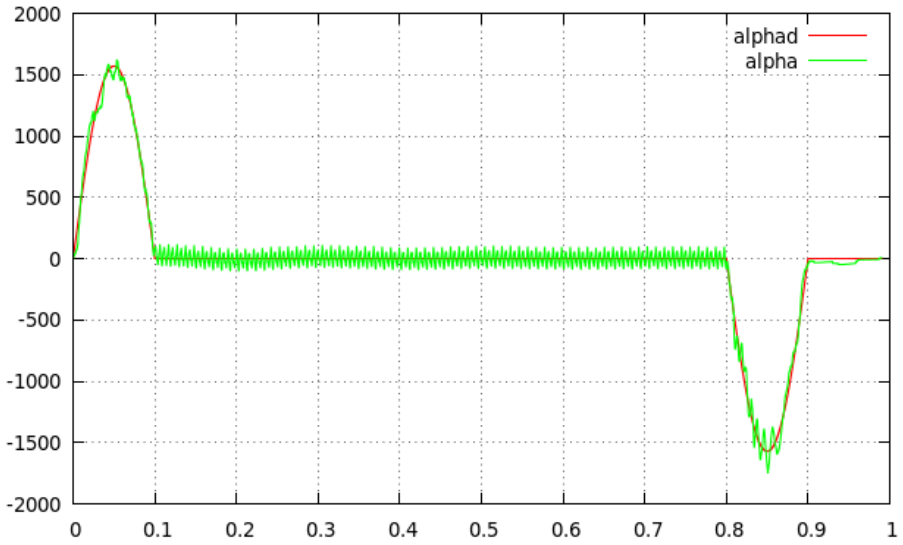

Figure 7: Plot of α_d vs motor α using analytical D/Q State-Space reference generation described by Equations 1 through 6 with motor parameter imbalances added.

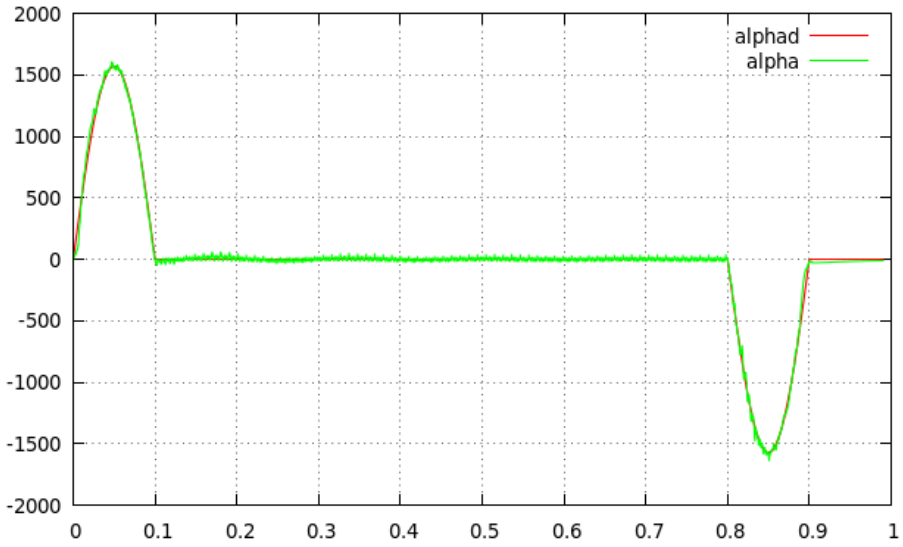

Figure 8: Plot of α_d vs motor α using a numerical State-Space reference generation described by Equations 7 through 14 with motor parameter imbalances added and equations compensated for these imbalances.

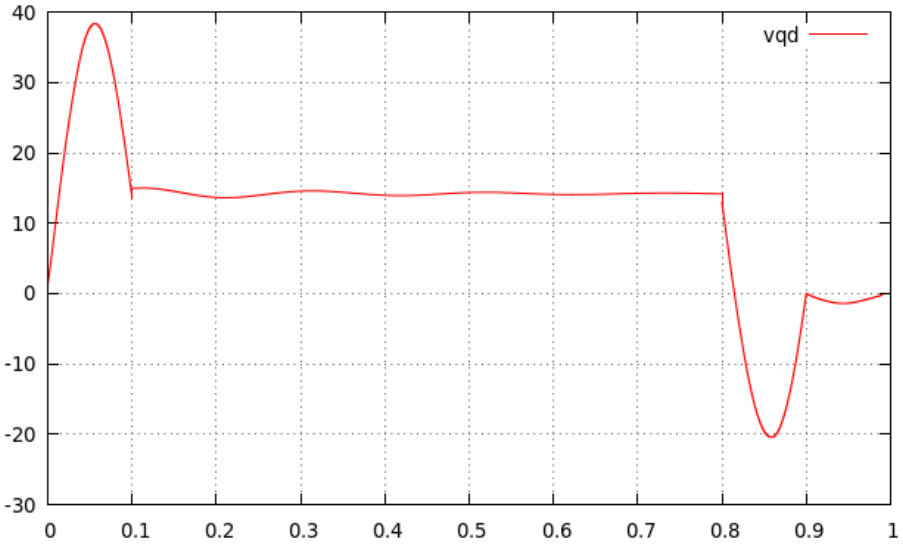

Figure 9: Plot of v_{qd} produced by Equation 6 with parameter imbalances added.

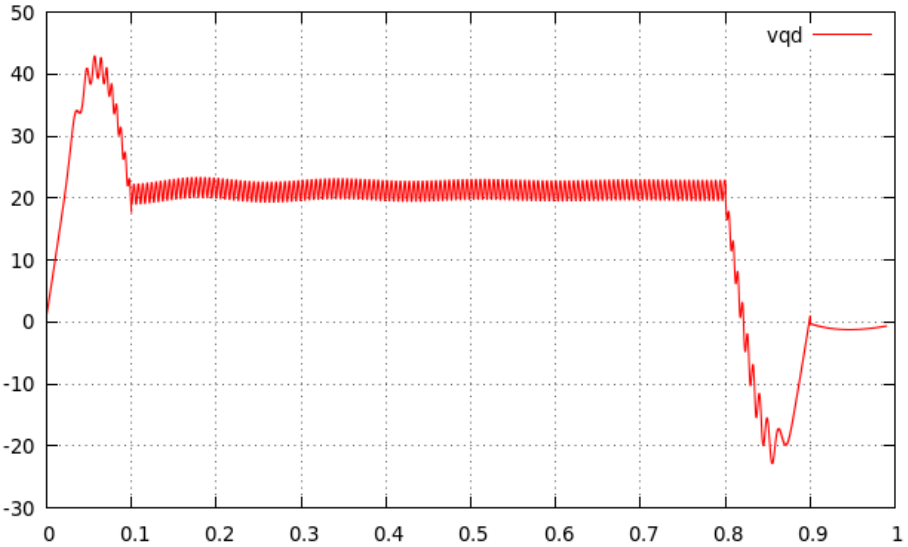

Figure 10: Plot of v_{qd} produced by Equation 14 with parameter imbalances added.

4 Disturbance Compensation for DC Bus Voltage Ripple

Rectified AC input power to the servo motor controller introduces yet another form of disturbance that is independent of motor characteristics and the reference generators described by the equations in Figure 1, 2, 3 and 4.

Up to this point, the tests described above (and those in other papers referenced by the author), applied a constant DC Bus voltage v_{bus} in all simulations presented. In servo control applications, this is not a realistic assumption for in most cases the DC bus to the amplifier is produced by simple AC voltage rectification from either a single phase or three phase voltage source[3]

To demonstrate how DC bus ripple and droop can be compensated we must first review the equations required to produce (generate) the Space Vector PWM waveforms used in this and other papers cited. This is described in an abbreviated form in Figures 11, 12, 13 and 14 below[4].

$$\sqrt{v_{dd}v_{dd} + v_{qd}v_{qd}} = vcmd_{mag} \tag{16}$$

$$\arctan v_{dd}/v_{qd} = vcmd_{ang} \tag{17}$$

Figure 11: Transformation of D/Q command voltages (reference Figure 1 or Figures 2 and 3 above) into Space Vector magnitude and angle quantities.

$$\theta_{actual}N_r + vcmd_{ang} = CtrlAngle \tag{18}$$

$$floor(3.0CtrlAngle/\pi) = SectorIndex \tag{19}$$

$$f(SectorIndex, sgn(CtrlAngle)) = SectorNumber \tag{20}$$

$$f(CtrlAngle, SectorIndex, sgn(CtrlAngle)) = SectorAngle \tag{21}$$

Figure 12: Using $vcmd_{mag}$ and $vcmd_{ang}$ determined in Figure 11 above the required intermediate calculations to determine voltage pulse positions applied to Phases A, B and C of the motor is made.

[3] In the US, a 60 Hz source voltage of 115, 230, or 480 VAC.

[4] A detailed description of Space Vector PWM generation is beyond the scope of this paper.

$$\frac{2}{3}T\_Z\sqrt{3}\sin(\pi\frac{SectorNumber}{3} - SectorAngle)\frac{vcmd_{mag}}{v_{bus}} = t_1 \quad (22)$$

$$\frac{2}{3}T\_Z\sqrt{3}\sin(SectorAngle - \frac{\pi}{3}(SectorNumber - 1))\frac{vcmd_{mag}}{v_{bus}} = t_2 \quad (23)$$

$$\frac{2}{3}T\_Z - t_1 - t_2 = t_0 \quad (24)$$

Figure 13: Details of the required calculations to determine voltage pulse time durations applied to Phases A, B and C of the motor from the intermediate calculates done in 12 above.

Referring to Figure 13 Time t_1 and t_2 are used in Equations 25 through 27 below to determine the duration of the SV voltage producing vectors. The time t_0 determines the *zero* vector. The quantity T_Z is the PWM time period.The quantity v_{bus} is the DC bus voltage of the power stage presumed to be a constant in the previous simulation runs.

With this information at hand, the final reference commands applied to the *triangle wave* carrier that determines switching frequency can be made. This is shown in 14 below.

$$f(SVTable\_a[SectorNumber], t_0, t_1, t_2, i_q, i_d) = v_a \quad (25)$$

$$f(SVTable\_b[SectorNumber], t_0, t_1, t_2, i_q, i_d) = v_b \quad (26)$$

$$f(SVTable\_c[SectorNumber], t_0, t_1, t_2, i_q, i_d) = v_c \quad (27)$$

Figure 14: Summary of functions required to determine the Motor Phase voltages v_a, v_b and v_c applied to Phases A, B and C of the motor. $SVTable\_a$, $SVTable\_b$ and $SVTable\_b$ are tables of predefined states used to select one of six sectors of the SV phasor diagram.

In Figure 14 v_a, v_b and v_c are the reference commands applied to a 1 PU triangle-wave reference that produce the control signals to the amplifier power stage (IPM power module). The quantities i_q and i_d are additional variables that can be used to control motor phase current ripple[5].

[5]Note: The discussion of D/Q feedback currents i_q and i_d as control variables to minimize motor phase current ripple is beyond the scope of this document.

To provide for a more accurate simulation, v_{bus} (which was set at constant of 200 VDC is the previous tests) is replaced by the bus voltage profile depicted in Figure 15 The ripple and droop shown in this figure occurs when motor is running through it's commanded profile with an established load that exceeds the reverse torque during deceleration.

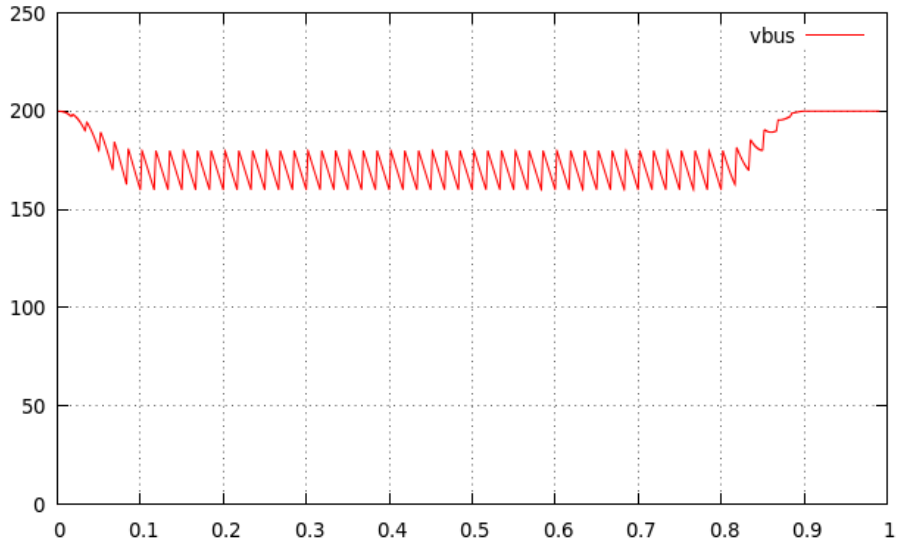

Figure 15: Plot of v_{bus} with voltage ripple and droop typically found on Servo Drives utilizing single phase AC line rectification into a electrolytic bus capacitor.

With the added disturbance from the ripple and droop of the the DC bus, the previous (motor parameter) compensated simulation run shown in Figure 8 now shows a less then idea reference tracking relationship in regards to commanded and actual α_d. This is because the simulation is run with v_{bus} in Equations 22 and 23 still set to a constant of 200 VDC. This is shown in Figure 16 below

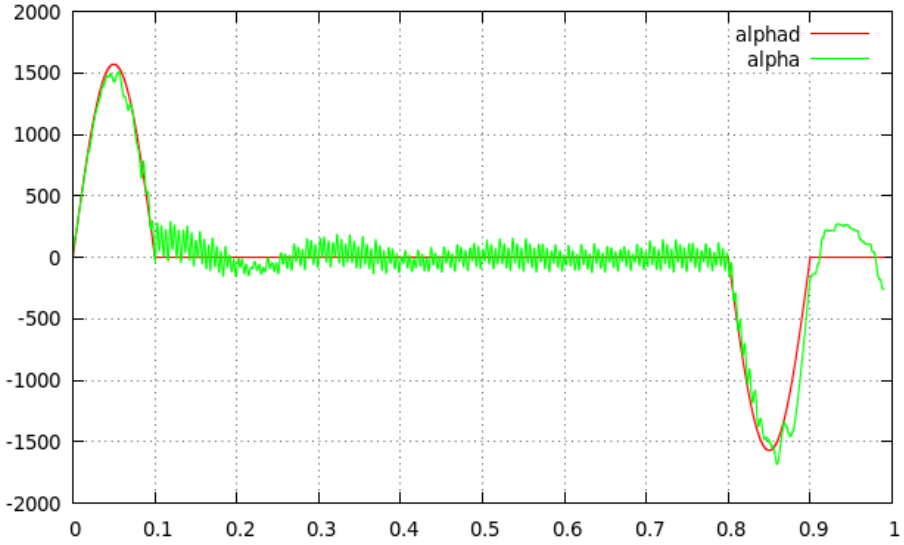

Figure 16: Plot of α_d vs motor α using a numerical State-Space reference generation described by Equations 7 through 14 with motor parameter imbalances added and equations compensated for these imbalances. Note that with v_{bus} ripple and droop now present on the DC bus, α becomes deformed again (compared to Figure 8.

With this change, the simulation shown in Figure 8 for the *compensated* numerical State-Space reference generation described by Equations 7 through 14 is re-run, but now with the added disturbance from the DC bus ripple and droop.

Now, if we feedback the measurement of the actual bus voltage in Figure 15 to the variable v_{bus} of Equations 22 and 23 of Figure 13 we have the DC Bus ripple/droop compensated and motor parameter imbalance compensated result shown in Figure 17 below.

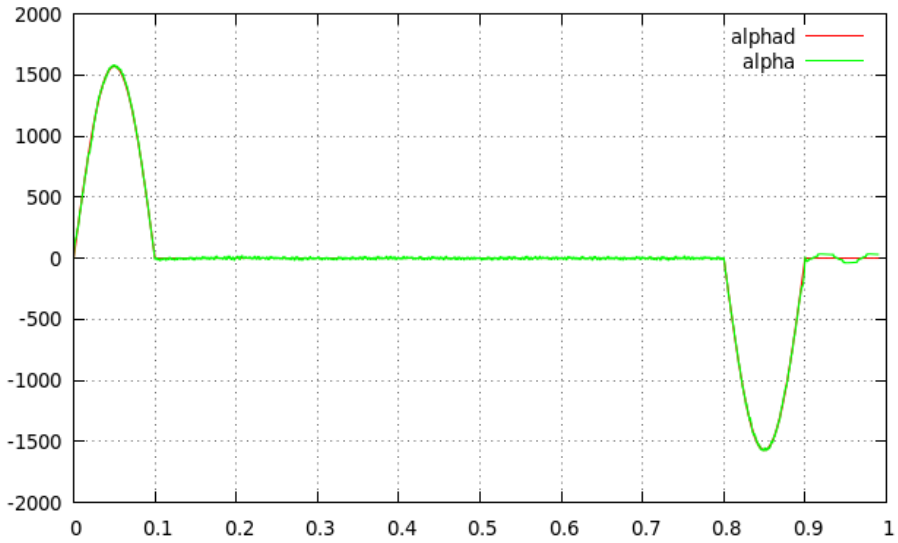

Figure 17: Plot of α_d vs motor α using a numerical State-Space reference generation described by Equations 7 through 14 with motor parameter imbalances added, and equations compensated for these imbalances. In addition the signal v_{bus} in Equations 22 and 23 compensated with the actual v_{bus} DC bus voltage shown in Figure 15.

The tracking error between α_d vs motor α again becomes small.

5 Summary

It has been shown that a traditional analytical reference for a state-space reference derived in the D/Q frame can be replaced with a numerically generated reference derived in the physical frame.

As shown the numerically generated method is more computationally intensive but provides the benefit of allowing the motor model to be characterized for the purposes of compensating an *unbalanced* system. Characterization of specific parameters can be accomplished using *least squares* or similar methods.

This paper showed examples for compensation of only three motor parameters. There are many more.

For instance J_m and B_m can be made functions of position. Also, we have assumed that the CEMF is purely sinusoidal. There is nothing to stop us from deriving a more realistic interpretation of say trapezoidal functions such as $trap(N_r\theta_d)$, $trap(N_r\theta_d - 2\pi/3)$ and $trap(N_r\theta_d - 4\pi/3)$.

In addition, it has been shown that for the numerically method (as well as the D/Q method) for reference generation can be improved by feeding back the the actual DC Bus voltage value to the Space Vector PWM control algorithm.

One particularly good example for the use of this approach is in the control of spindle motors where motor (or load) unbalances can cause deleterious effects in performance. This and the use of the control signal i_q and i_d mentioned briefly in Figure 14 above to control ripple current will be presented in a future paper.

References

[1] Marc Bodson, John N. Chiasson, Robert T. Novotnak and Ronold B. Rekoswski
High Performance Nonlinear Feedback Control of a Permanent Magnet Stepping Motor.
First IEEE Conference on Control Applications, 1992. ISBN 0-7803-0047-5.

[2] *Implementation of an Advanced AC Brushless Motor Controller for Use in High Reliability Applications*
Michael E. Aiello, April 2 2016.
`https://meaconsultingdotorg.files.wordpress.com/2015/12/controller.pdf`

Revision History

Revision	Date	Author(s)	Description
1.0	August 9, 2020	MEA	Created
1.1	July 25, 2021	MEA	Added description of method for DC bus rippple compensation.